



Article

A Mechanical Model for Stress Relaxation of Polylactic Acid/Thermoplastic Polyurethane Blends

Yi-Sheng Jhao ¹, Hao Ouyang ¹, Chien-Chao Huang ², Fuqian Yang ³ and Sanboh Lee ^{1,*}

¹ Department of Materials Science and Engineering, National Tsing Hua University, Hsinchu 300, Taiwan

² College of Semiconductor Research, National Tsing Hua University, Hsinchu 300, Taiwan

³ Materials Program, Department of Chemical and Materials Engineering, University of Kentucky, Lexington, KY 40506, USA

* Correspondence: sblee@mx.nthu.edu.tw; Tel.: +886-3-5719677

Abstract: Polylactic acid (PLA) is considered a promising biodegradable polymer alternative. Due to its high brittleness, composite materials made by melt blending thermoplastic polyurethane (TPU) with PLA can enhance the toughness of PLA. To understand the forced aging caused by stress relaxation in polymer materials, this study explains the stress relaxation experiments of PLA/TPU blends with different mass ratios under applied strain through mechanical model simulations. The Kelvin representation of the standard linear solid model (SLSM) is used to analyze the stress relaxation data of TPU/PLA blends, successfully explaining that the Young's moduli (E_1 and E_2) of springs decrease with increasing temperature and TPU content. The viscosity coefficient of the PLA/TPU blends decreases with increasing temperature, and its reciprocal follows the Arrhenius law. For TPU/PLA blends with increased concentration of TPU, the activation energy for stress relaxation shows a linear decrease, confirmed by the glass transition point measured by DMA, indicating that it does not involve chemical reactions.

Keywords: stress relaxation; Polylactic acid; thermoplastic polyurethane; Kelvin representation; standard linear solid model



Citation: Jhao, Y.-S.; Ouyang, H.; Huang, C.-C.; Yang, F.; Lee, S. A Mechanical Model for Stress Relaxation of Polylactic Acid/Thermoplastic Polyurethane Blends. *J. Compos. Sci.* **2024**, *8*, 169. <https://doi.org/10.3390/jcs8050169>

Academic Editor: Francesco Tornabene

Received: 2 March 2024

Revised: 26 April 2024

Accepted: 29 April 2024

Published: 1 May 2024



Copyright: © 2024 by the authors. Licensee MDPI, Basel, Switzerland. This article is an open access article distributed under the terms and conditions of the Creative Commons Attribution (CC BY) license (<https://creativecommons.org/licenses/by/4.0/>).

1. Introduction

Aging is an undesirable process for polymeric materials, but it is inevitable. Stress relaxation of polymeric material is a kind of forced aging, which is often simulated by the mechanical model. The mechanical model consisting of springs and dashpots is often used to understand the deformation mechanism of the long-term forced aging problem of polymeric materials. The simplest mechanical models are the Maxwell and Voigt models, where the former and the latter are spring and dashpot connected in series and parallel, respectively. More complex models are the standard linear solid model (SLSM) with three elements [1] and the Burgers model with four elements [2]. Burgers and SLSM models described the creep recovery, and stress relaxation behaviors, respectively. Furthermore, the real polymeric materials cannot be described by the model with a few dashpots and springs [3]. The Maxwell–Weichert model with Maxwell elements connected in parallel was proposed to explain the stress relaxation experiment [4,5]. In addition to the mechanical model, an empirical equation was also applied to analyze the stress relaxation phenomenon of polymeric materials. Fancey [6] utilized the Kohlrausch–Williams–Watts (KWW) function based on the Weibull distribution function to represent the viscoelastic change of the stress relaxation experiment. His idea arises from the Weibull function, often used to explain mechanical failure [7].

Polylactic acid (PLA) has been considered a promisingly biodegradable alternative to traditional petro-polymers due to its attractive mechanical properties, high renewability, good biodegradability, and relatively low cost [8]. Pelouze [9] was the first to prepare low molecular weight PLA using the condensing L-lactic acid and removing water constantly.

Sosnowski et al. [10] obtained high molecular weight PLA via ring-opening polymerization (ROP) of lactide with protic compounds as initiators and tin (II) octoate ($\text{Sn}(\text{Oct})_2$) as a catalyst. The properties of PLA are affected more by the chiral carbon in lactic acid than by the molecular weight of PLA. PLA with different concentrations of L-Isomer and D-Isomer can be semi-crystalline or amorphous, which has a melting point ca. 175 °C and a glass transition point ca. 55–60 °C [11].

Although PLA has better mechanical properties than commodity polymers such as polystyrene, polyethylene, and polyethylene terephthalate [12], it is brittle, has low impact strength, and has a low crystallization degree. PLA-based composites and PLA-based polymer blends are the solutions to enhance the mechanical properties. Raquez et al. [13] classified nanocomposites as plate-like nanofillers (1D), nanofibers (2D), and nanoparticles (3D). Tokoro et al. [14] mixed the PLA with bamboo fibers to form a PLA/bamboo composite, which has greater bending strength and impact strength than pristine PLA at 25 °C. Metta et al. [15] used Hakee Rheomix to prepare a PLA and polycaprolactone (PCL) blend. They found that the PLA/PCL blend increases the elongation, impact strength, and loss factor, and decreases the modulus and strength of the PLA/PCL blend by increasing the concentration of PCL up to 20% PCL. Furthermore, Takayama and Todo [16] used lysine triisocyanate (LTI) as an additive to PLA/PCL blends to enhance the miscibility of PLA/PCL so that PLA/PCL has better tensile strength and impact strength. Ho et al. [17] prepared the thermoplastic polyolefin elastomer-graft-poly lactide by reacting poly lactide with maleic anhydride-functionalized TPD (TPD-MAH) in the presence of 4-dimethylaminopyridine (DMP). The formed PLA/TPO blend has a larger elongation at break, tensile toughness, and Izod impact strength than pristine PLA, but lower tensile strength and tensile modulus than the latter. Tsai et al. [18] prepared the PLA/PMMA (polymethyl methacrylate) blend by hot-press method at 190 °C under compression stress of 1.96 MPa. They studied the effect of UV irradiation on physical aging via DSC.

Thermoplastic polyurethane (TPU), owning excellent elastic properties, high transparency, great toughness, and biocompatibility is a potential candidate for implanted devices [19]. Li and Shimizu [20] found that melt blending of TPU with PLA can enhance the toughness of PLA. Jhao et al. [2] reported that when temperature is high, the activation energies for the steady-state creep and transient creep of PLA/TPU blends decrease linearly with the increase in the concentration of TPU. In addition to the creep, when the temperature is high enough, the stress relaxation behavior also occurs frequently in the polymeric materials. This prompted us to investigate the effect of TPU concentration on the stress relaxation behavior of PLA/TPU blends. We proposed the Kelvin representation of the standard linear solid model to describe the stress relaxation of PLA/TPU blends. The existing models are also discussed.

2. Experimental

The PLA 4032D with T_g ca. 55–60 °C and TPU 8785A with 300-grade were purchased from Nature Works LLC (Minnetonka, MN, USA) and Bayer Co, Ltd. (Leverkusen, Germany), respectively. The former has a melting point of 155–170 °C, and the latter melting point is 160–180 °C. The PLA was a semi-crystalline polymer with 98% L-isomer and 2% D-isomer. The chemical structures of polylactide (PLA) and thermoplastic polyurethane (TPU) are shown in Figure 1a,b, respectively.

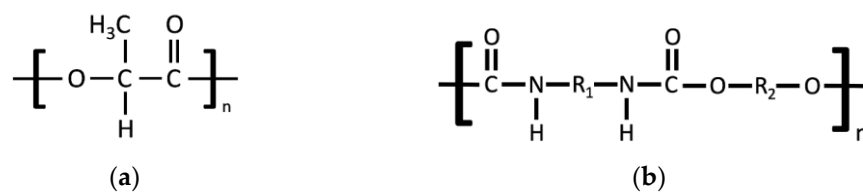


Figure 1. The chemical structures of (a) polylactide (PLA) and (b) thermoplastic polyurethanes (TPU).

Pristine PLA and TPU, and PLA/TPU blends with 30/70, 50/50, and 70/30 mass ratios were fabricated via a melting blend method at 200 °C [2]. Briefly, the PLA and TPU mixture was dried in an oven at 80 °C for 4 h and moved to an injection molding machine at the injection molding point of 200 °C. The PLA/TPU blend was injected into a mold to form a thin plate where the molding temperature and pressure were 30 °C and 2.94 MPa, respectively. The dumb-bell-shape specimens with a gauge length of 9.7 mm, width of 1.5 mm, and thickness of 0.7 mm were laser-cut from the thin plate. After grinding on 400, 800, 1200, and 2500 grit CarbiMet papers and polishing with 1 µm alumina slurries, the specimens were annealed at 50 °C for one day. Then, the furnace was cooled down to 25 °C to relax the residual stress arising from the sample preparation.

The stress relaxation was performed with a TA 800 dynamic mechanical analyzer (DMA) (TA Instrument Co., Ltd., New Castle, DE, USA). Because of instrument limitations, the stress relaxations of PLA/TPU blends of different ratios of PLA to TPU were operated under different applied strains. The specimens were maintained at a preset temperature for at least 5 min to reach thermal equilibrium, stretched to a specific elongation, and kept the same strain for 60 min. The stress as a function of time was recorded. The glass transition temperature was performed at a temperature range from −80 °C to 110 °C at a heating rate of 5 °C/min with a frequency of 1 Hz using a TA 800 dynamic mechanical analyzer (DMA) (TA Instrument Co., New Castle, DE, USA).

3. Results

Using DMA, we measure the glass transition temperatures of the prepared PLA/TPU blends. Figure 2 shows the curves of $\tan(\delta)$ versus temperature for PLA/TPU blends with different ratios of PLA to TPU. The temperatures of the right and left peaks in the figure correspond to the glass transition temperatures of PLA and TPU, respectively. From Figure 2, we obtained the glass transition temperatures of the PLA/TPU blends listed in Table S1. The glass transition temperature of PLA decreases slightly with increasing the TPU concentration of the PLA/TPU blend, but the trend of the glass transition temperature of TPU versus temperature is the opposite.

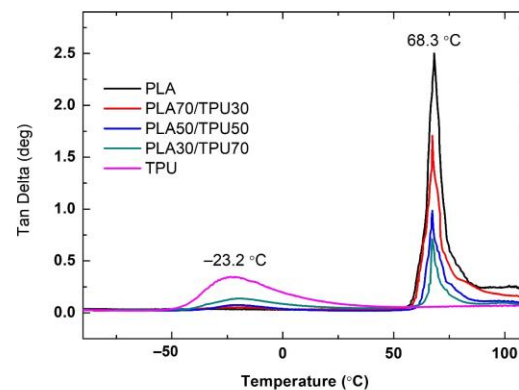


Figure 2. The curves of $\tan(\delta)$ versus temperature for the PLA/TPU blends with different ratios of PLA to TPU.

Figure 3 shows the stress relaxation of PLA/TPU blends with 70/30 for the mass ratio of PLA to TPU under different strains at temperatures of 10, 20, 30, and 40 °C. For a given strain and temperature, the stress decreases rapidly with time, and its slope changes slowly until it reaches a steady state. For a given time and strain, the stress increases with increasing temperature. Figure S1–S4 in Supplementary Information illustrate the stress relaxation of PLA/TPU blends with 100/0, 50/50, 30/70, and 0/100 for the mass ratio of PLA to TPU under different applied strains at 10–40 °C, respectively. They have a similar trend to the PLA/TPU blend with 70/30 for the mass ratio of PLA to TPU. For the same applied strain and temperature, the stress at a given time is larger for the specimen with the smaller mass ratio of PLA to TPU.

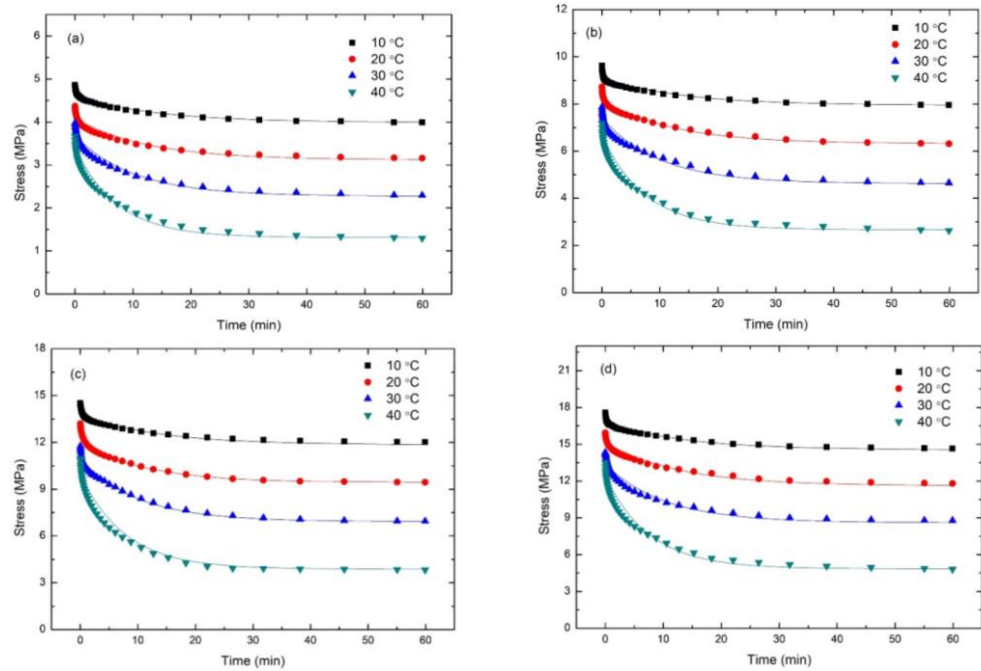


Figure 3. The stress relaxation of PLA/TPU blend with mass ratio of PLA to TPU: 70/30 at different temperatures under applied strain of (a) 0.3%, (b) 0.6%, (c) 0.9%, and (d) 1.1%.

Here, R^2 is a confidential interval composed of an upper bound and a lower bound denoting the range within which the estimate would be expected to fall if resampled.

4. Discussion

The Kelvin representation of the standard linear solid model (SLSM) is used to analyze the stress relaxation data of TPU/PLA blends. The Kelvin representation of SLSM consists of spring 1 with Young’s modulus E_1 connected with the Kelvin–Voigt element of Young’s modulus E_2 and viscosity coefficient η_2 in series, as shown in Figure 4. The stress $\sigma(t)$ of Kelvin representation of SLSM for a given strain ε is written as

$$\sigma(t) = \frac{E_1 E_2 \varepsilon}{E_1 + E_2} + \frac{E_1^2 \varepsilon}{E_1 + E_2} \exp\left(-\frac{(E_1 + E_2)t}{\eta_2}\right) \quad (1)$$

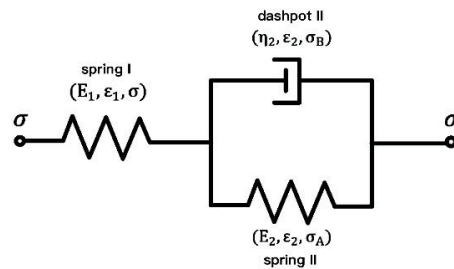


Figure 4. The schematic of Kelvin representation of the standard linear solid model.

The solid lines in Figure 3 and Figures S1–S4 in Supplementary Information are obtained using Equation (1) with the mechanical constants E_1 , E_2 , and η_2 listed in Table 1 and Tables S2–S5 in Supplementary Information. E_1 and E_2 decrease with increasing temperature for all PLA/TPU blends. E_1 and E_2 decrease with increasing concentration of TPU in PLA/TPU blend. The viscosity coefficient decreases with increasing temperature, and its reciprocal follows the Arrhenius plot, as shown in Figure 5. The viscosity coefficient increases with the TPU content of the PLA/TPU blend. From the slope of Figure 5, we obtain the activation energy of stress relaxation of the PLA/TPU blend, as shown in Figure 6. According to Figure 6, the activation energy of stress relaxation decreases linearly with

the increasing TPU content of the TPU/PLA blend, which is not involved in the chemical reaction, indicating that the two components of the system are immiscible and consistent with the reports in the literature [21–23]. This phenomenon was supported by the glass transition point measured by DMA. Table S1 in Supplementary Information shows the glass transition points T_g of the PLA and TPU are 68.3 and -23.2 °C, respectively. The two T_g of PLA/TPU polymer blend are shown in Table S1 in Supplementary Information. One is near 68.3 °C, and the other -23.2 °C. That confirms the immiscibility between PLA and TPU.

Table 1. SLSM mechanical constants E_1 , E_2 , and η_2 of PLA/TPU blend with 70/30 for the mass ratio of PLA to TPU at different temperatures.

Temperature	10 °C	20 °C	30 °C	40 °C
E_1 (GPa)	1.53 ± 0.07	1.37 ± 0.07	1.22 ± 0.08	1.12 ± 0.04
E_2 (GPa)	10.2 ± 0.4	4.53 ± 0.24	2.08 ± 0.09	0.722 ± 0.31
η_2 (GPa·min)	160 ± 10	71.6 ± 2.6	33.3 ± 1.2	13.9 ± 0.7
R^2	0.974	0.982	0.991	0.980

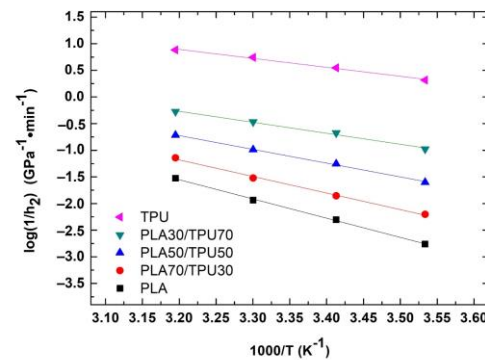


Figure 5. The plot of $\log(1/\eta_2)$ versus $1/T$ for PLA/TPU blends with different mass ratios of PLA to TPU.

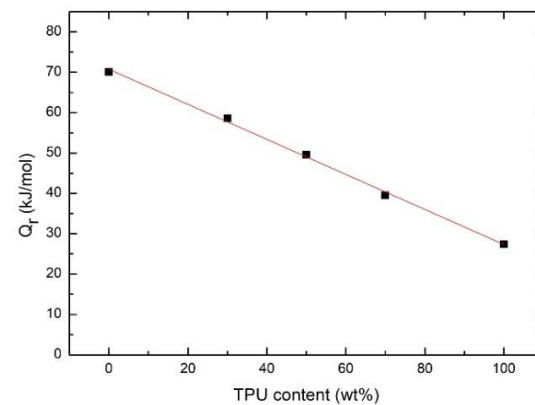


Figure 6. Activation energies (Q_r) of stress relaxation of PLA/TPU blends with different contents of TPU.

According to probability and statistics, the Weibull distribution function is a continuous probability distribution commonly applied to material reliability and failure analysis. Fancy [24] used the Kohlrausch–Williams–Watts (KWW) function based on the Weibull distribution to analyze the stress relaxation data of nylon 6, 6 fiber. The KWW function is empirical, which is expressed as

$$\sigma(t) = E_{KWW1}\varepsilon + E_{KWW2}\varepsilon \exp[-(t/\tau_{KWW})^{\beta_{KWW}}] \tag{2}$$

where E_{KWW1} and E_{KWW2} are the Young’s moduli, and ε is the applied strain. τ and β are relaxation time and shape parameter, respectively.

Equation (2) equals Equation (1) if the following equations are satisfied.

$$E_{KWW1} = \frac{E_1 E_2}{E_1 + E_2} \tag{3}$$

$$E_{KWW2} = \frac{E_1^2}{E_1 + E_2} \tag{4}$$

$$\frac{1}{\tau_{KWW}} = \frac{E_{KWW2}}{\eta_{KWW2}} = \frac{E_1 + E_2}{\eta_2} \text{ if } \beta_{KWW} = 1 \tag{5}$$

Equations (3) and (4) are obtained from the equality of Equations (1) and (2) at time infinity and the initial time, respectively, and Equation (5) is from that of the exponential terms in Equations (1) and (2).

The solid lines in Figure 7 were obtained using Equation (2) with the mechanical parameters listed in Table 2, where the symbols represent the stress relaxation data of the PLA/TPU blend with 50/50 for the mass ratio of PLA to TPU under an applied strain of 1.2% at different temperatures. The solid lines in Figure S2c in Supplementary Information were obtained using Equation (1) with the mechanical parameters listed in Table S3 in Supplementary Information, where the experimental data are the same as those in Figure 7. According to Table 2, the confidential interval R^2 of the KWW function is comparable to that of SLSM. However, the former uses four mechanical parameters to curve fit, and the latter uses three. The difference in the confidential intervals using the SLSM and KWW models is due to β_{KWW} being 0.91~0.79, not 1. Furthermore, the parameter β_{KWW} in Equation (2) has no physical meaning. The value of E_{KWW1} decreases with increasing temperature, but that of E_{KWW2} has the opposite trend of decreasing temperature. Young’s modulus with an increasing temperature function violates the concept of polymeric materials [6,25]. Therefore, we do not recommend the KWW model to simulate the polymer’s stress relaxation behavior.

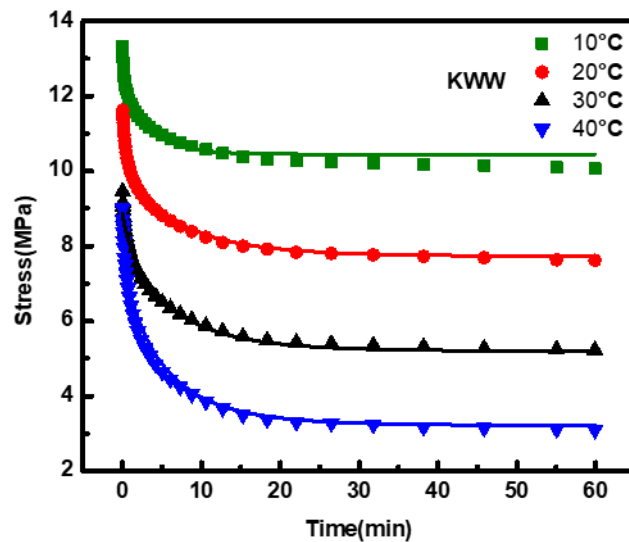


Figure 7. The stress relaxation data of the PLA/TPU blend with 50/50 for the mass ratio of PLA to TPU under the applied strain of 1.2% are curve-fitted by the KWW model.

Table 2. The mechanical parameters of the KWW model to fit the stress relaxation of PLA/TPU blend with 50/50 for the mass ratio of PLA to TPU under the applied strain of 1.2%.

Temperature	10 °C	20 °C	30 °C	40 °C
E_{KWW1} (MPa)	836	644	433	268
E_{KWW2} (MPa)	176	257	305	397
η_{KWW2} (MPa·min)	533	1311	1586	1826
τ_{KWW} (min)	3.03	5.1	5.20	4.6
β_{KWW}	0.91	0.76	0.80	0.79
R^2	0.943	0.969	0.980	0.968

Heuchel et al. [4] used the modified Maxwell–Weichert model to describe the stress relaxation phenomenon of amorphous shape-memory polymers. The modified Maxwell–Weichert model consists of spring 1 and Maxwell elements 2 and 3 connected in parallel and can be expressed as

$$\sigma(t) = E_{MW1}\varepsilon + E_{MW2}\varepsilon\exp(-t/\tau_{MW2}) + E_{MW3}\varepsilon\exp(-t/\tau_{MW3}) \tag{6}$$

where E_{MW1} , E_{MW2} , and E_{MW3} are the Young’s moduli of springs 1, 2, and 3, and ε is the applied strain. τ_{MW2} and τ_{MW3} are the relaxation times of Maxwell elements 2 and 3. Note τ_{MW2} and τ_{MW3} are related to viscosity coefficients as

$$\tau_{MWi} = \eta_{MWi}/E_{MWi} \tag{7}$$

where i can be 2 and 3 to represent dashpots of Maxwell elements 2 and 3, respectively. Comparing Equation (1) with Equation (6), we find that

$$\frac{E_1 E_2}{E_1 + E_2} = E_{MW1} \tag{8}$$

$$E_1 = E_{MW1} + E_{MW2} + E_{MW3} \tag{9}$$

Note that Equations (8) and (9) are obtained from the equality of Equations (1) and (6) at time infinity and the initial time, respectively.

The solid curves in Figure 8 were obtained using Equation (6) with the mechanical parameters listed in Table 3, where the symbols represent the stress relaxation data of the PLA/TPU blend with 50/50 for the mass ratio of PLA to TPU under the applied strain of 1.2% at different temperatures. It can be seen from Tables 2 and 3 that E_1 , E_2 , E_{KWW1} , E_{KWW2} , E_{MW1} , E_{MW2} , and E_{MW3} follow Equations (3), (4), (8), and (9). The Maxwell–Weichert model has the largest confidential interval R^2 among the above three models because it has five mechanical parameters to curve-fit the experimental data. According to Table 3, the value of E_{MW1} decreases with increasing temperature, but the values of E_{MW2} and E_{MW3} have a random relation with the temperature. Young’s modulus as a random relation with temperature violates the concept of polymeric materials [6,25]. Therefore, the Maxwell–Weichert model is unsuitable for simulating the polymer’s stress relaxation behavior.

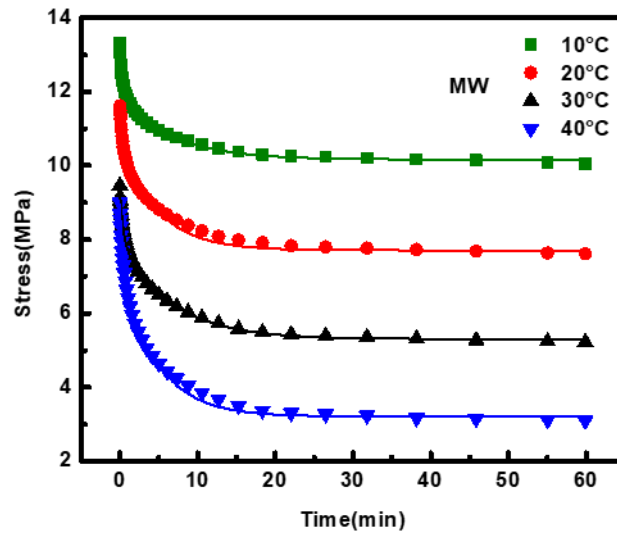


Figure 8. The stress relaxation data of the PLA/TPU blend with 50/50 for the mass ratio of PLA to TPU under the applied strain of 1.2% are curve-fitted by the Maxwell–Weichert model.

Table 3. The mechanical parameters of the Maxwell–Weichert model to fit the stress relaxation of PLA/TPU blend with 50/50 for the mass ratio of PLA to TPU under the applied strain of 1.2%.

Temperature	10 °C	20 °C	30 °C	40 °C
E_{MW1} (MPa)	847	642	442	267
E_{MW2} (MPa)	149	252	222	342
η_{MW2} (MPa·min)	978	1189	1460	1594
E_{MW3} (MPa)	102	79	102	137
η_{MW3} (MPa·min)	33.7	15.0	47.4	37.0
τ_{MW2} (min)	6.56	4.72	6.58	4.66
τ_{MW3} (min)	0.33	0.19	0.46	0.27
R^2	0.997	0.992	0.998	0.997

Instead of the Kelvin representation of SLSM, the Maxwell representation of SLSM can also fit the stress relaxation data of PLA/TPU blends with different mass ratios of PLA to TPU. The Maxwell representation of SLSM consists of spring 1 connected with the Maxwell element 2 in parallel. Ju et al. [1] obtained the solution of stress relaxation of polymeric materials using the Maxwell representation of SLSM as

$$\sigma(t) = E_{M1}\varepsilon + E_{M2}\varepsilon \exp(-E_{M2}t/\eta_{M2}) \tag{10}$$

$$\tau_M = \eta_{M2}/E_{M2} \tag{11}$$

where E_{M1} and E_{M2} are Young’s moduli of springs 1 and 2, respectively. η_{M2} is the viscosity coefficient of dashpot 2 and τ_M is the relaxation time of Maxwell representation. Equation (10) is identical to Equation (1) if the following equations are satisfied.

$$E_{M1} = \frac{E_1 E_2}{E_1 + E_2} \tag{12}$$

$$E_{M2} = \frac{E_1^2}{E_1 + E_2} \tag{13}$$

$$\eta_{M2} = \left(\frac{E_1}{E_1 + E_2} \right)^2 \eta_2 \tag{14}$$

Equations (12) and (13) are obtained from the equality of Equations (1) and (10) at time infinity and the initial time, respectively, and Equation (13) is from that of the exponential terms in Equations (1) and (10).

Using Equations (12)–(14) and Table S2 in Supplementary Information, we obtain the E_{M1} , E_{M2} , and η_{M2} of PLA/TPU blends with 50/50 for the mass ratio of PLA to TPU, listed in Table 4. According to Table 4, E_{M1} decreases with increasing temperature, but E_{M2} increases with increasing temperature. Young's modulus of spring 2 (Maxwell element) increases with increasing temperature, violating the polymeric material concept. Lagakos et al. [25] and Ferry [6] illustrated that the amorphous polymer has the trend of Young's modulus decreasing temperature function. Therefore, the Maxwell representation of SLSM cannot be used to describe the stress relaxation behavior of the PLA/TPU blend.

Table 4. The mechanical parameters of Maxwell representation of the SLSM for the stress relaxation of PLA/TPU blend with 50/50 for the mass ratio of PLA to TPU.

Temperature	10 °C	20 °C	30 °C	40 °C
E_{M1} (GPa)	0.823 ± 0.038	0.634 ± 0.027	0.444 ± 0.023	0.278 ± 0.019
E_{M2} (GPa)	0.176 ± 0.011	0.257 ± 0.011	0.305 ± 0.012	0.398 ± 0.021
η_{M2} (GPa·min)	1.31 ± 0.06	1.50 ± 0.08	1.61 ± 0.07	1.80 ± 0.08

The above analyses reveal that the KWW model, the Maxwell–Weichert model, and the Maxwell representation of SLSM led to incompetent trend, which is physically unsound. Such a result likely indicates that these methods do not “correctly” connect with the microstructure of the PLA/TPU blends and the use of the relaxation parameters (times and index). In general, it requires the correct formulation to catch up the main deformation mechanisms if possible.

5. Summary and Conclusions

Stress relaxation experiments were conducted on PLA/TPU blends with varying mass ratios under applied strain. This study utilized the Kohlrausch–Williams–Watts (KWW) function of the Weibull distribution and the Maxwell expression of the standard linear solid model (SLSM) to analyze the stress relaxation data at different PLA to TPU mass ratios, finding that the Young's modulus increased with temperature. However, if converted to the Maxwell–Weichert model, the relationship between Young's modulus and temperature appeared random. The Young's modulus of the three models contradicts the concept of polymer materials. Compared to the Kelvin representation of the SLSM used for analyzing the stress relaxation data of TPU/PLA blends, Young's moduli (E_1 and E_2) of all PLA/TPU blends decreased with the temperature. Additionally, E_1 and E_2 decreased as the concentration of TPU in the PLA/TPU blends increased. The viscosity coefficient of the PLA/TPU blends decreased with increasing temperature, and its reciprocal followed the Arrhenius law. The viscosity coefficient increased with the TPU concentration in the PLA/TPU blends. As the TPU content in the TPU/PLA blends increased, the activation energy for stress relaxation linearly decreased, a phenomenon not involving chemical reactions, supported by DMA measurements of the glass transition point, confirming the incompatibility between PLA and TPU.

Supplementary Materials: The following supporting information can be downloaded at: <https://www.mdpi.com/article/10.3390/jcs8050169/s1>, Figures S1–S4: The stress relaxations of PLA/TPU composites of different concentrations of TPU, Table S1. The glass transition temperatures of Tg,1 and Tg,2 of PLA/TPU blends with different ratios of PLA to TPU, Table S2. SLSM mechanical constants E_1 , E_2 , and η_2 of PLA, Table S3. SLSM mechanical constants E_1 , E_2 , and η_2 of PLA/TPU blend with 50/50 for the mass ratio of PLA to TPU. Table S4. SLSM mechanical constants E_1 , E_2 , and η_2 of PLA/TPU blend with 30/70 for the mass ratio of PLA to TPU at different temperatures. Table S5. SLSM mechanical constants E_1 , E_2 , and η_2 of TPU (or 0/100 for the mass ratio of PLA to TPU) at different temperatures.

Author Contributions: Y.-S.J.: Verification, data curation, writing original draft; H.O.: formal analysis, methodology, project administration, writing—reviewing, and editing; C.-C.H.: formal analysis, data curation, validation; F.Y.: verification, writing—reviewing and editing; S.L.: supervision, funding acquisition, project administration, writing—reviewing and editing. All authors have read and agreed to the published version of the manuscript.

Funding: We thank the National Science and Technology Council, Taiwan, through grant number NSTC 112-2221-E-007-038 for the financial support.

Data Availability Statement: Data are available for request.

Conflicts of Interest: The authors declare no conflicts of interest.

References

1. Ju, Y.C.; Chiang, D.; Tsai, M.Y.; Ouyang, H.; Lee, S. Stress Relaxation Behavior of Poly(Methyl Methacrylate)/Graphene Composites: Ultraviolet Irradiation. *Polymers* **2022**, *14*, 41922. [[CrossRef](#)] [[PubMed](#)]
2. Jhao, Y.S.; Ouyang, H.; Yang, F.; Lee, S. Thermo-Mechanical and Creep Behavior of Polylactic Acid/Thermoplastic Polyurethane Blends. *Polymers* **2022**, *14*, 5276. [[CrossRef](#)] [[PubMed](#)]
3. Lakes, R.S.; Solid, V. *CRC Mechanical Engineering Series*; CRC Press: Boca Raton, FL, USA, 1993.
4. Heuchel, M.; Chi, J.; Kratz, K.; Kosmella, H.; Lendlein, A. Relaxation Based Modeling of Tunable Shape Recovery Kinetics Observed under Isothermal Conditions for Amorphous Shape-Memory Polymers. *Polymer* **2010**, *51*, 6212–6218. [[CrossRef](#)]
5. Aklonis, J.J.; Macknight, W.J. *Introduction to Polymer Viscoelasticity*, 2nd ed.; Wiley: New York, NY, USA, 1983.
6. Ferry, D. *Viscoelastic Properties of Polymers*, 3rd ed.; Wiley: New York, NY, USA, 1980.
7. Wong, T.-F.; Wong, R.H.C.; Chau, K.T.; Tang, C.A.; Statistics, M. Weibull Distribution and Micromechanical Modeling of Compressive Failure in Rock. *Mech. Mater.* **2006**, *38*, 664–681. [[CrossRef](#)]
8. Drumright, R.E.; Gruber, P.R.; Henton, D.E. Polylactic Acid Technology. *Adv. Mater.* **2000**, *12*, 1841–1846. [[CrossRef](#)]
9. Carothers, W.H.; Dorough, G.L.; van Natta, F.J. Studies of Polymerization and Ring Formation. X. The Reversible Polymerization of Six-Membered Cyclic Esters. *J. Am. Chem. Soc.* **1932**, *54*, 701–772. [[CrossRef](#)]
10. Sosnowski, S.; Gadzinowshi, M.; Slowkowshi, S. Poly (L, L-lactide) Microspheres by Ring-Opening Polymerization. *Macromolecules* **1996**, *29*, 4556–4564. [[CrossRef](#)]
11. Stridsberg, K.; Ryner, K.; Albertsson, A.C. Controlled Ring-Opening Polymerization: Polymers with Designed Macromolecular Architecture. *Adv. Polym. Sci.* **2002**, *157*, 4565.
12. Sudesh, K.; Iwata, T. Sustainability of biobased and biodegradable plastics. *Clean-Soil Air Water* **2008**, *36*, 433–442. [[CrossRef](#)]
13. Raquez, J.-M.; Habibi, Y.; Murariu, M.; Dubois, P. Polylactic acid (PLA)-based nanocomposites. *Prog. Polym. Sci.* **2013**, *38*, 1504–1542. [[CrossRef](#)]
14. Tokoro, R.; Vu, D.M.; Okubo, K.; Fujii, T.; Fujiura, T. How to improve mechanical properties of polylactic acid with bamboo fibers. *J. Mater. Sci.* **2008**, *43*, 775–787. [[CrossRef](#)]
15. Matta, K.; Rao, R.U.; Suman, K.N.S.; Rambabu, V. Preparation and Characterization of Biodegradable PLA/PCL Polymeric Blends. *Procedia Mater. Sci.* **2014**, *6*, 1226–1270. [[CrossRef](#)]
16. Takayama, T.; Todo, M. Improvement of impact fracture properties of PLA/PCL polymer blend due to LTI addition. *J. Mater. Sci.* **2006**, *41*, 4989–4992. [[CrossRef](#)]
17. Ho, C.H.; Wang, C.H.; Lin, C.I.; Lee, Y.D. Synthesis and characterization of TPO-PLA copolymer and its behavior as compatibilizer for PLA/TPO blends. *Polymer* **2008**, *49*, 3902–3910. [[CrossRef](#)]
18. Tsai, M.H.; Ouyang, H.; Yang, F.; Wei, M.K.; Lee, S. Effects of ultraviolet irradiation on the aging of the blends of Poly(lactide acid) and Poly(methyl methacrylate). *Polymer* **2022**, *252*, 124947. [[CrossRef](#)]
19. Jing, X.; Mi, H.Y.; Peng, X.F.; Turng, L.S. The Morphology, properties, and shape memory behavior of polylactic acid/thermoplastic polyurethane blends. *Polym. Eng. Sci.* **2015**, *55*, 70–80. [[CrossRef](#)]
20. Li, Y.; Shimizu, H. Toughening of polylactic acid by melting blending with a biodegradable poly(ethyl)urethane elastomer. *Macromol. Biosci.* **2007**, *7*, 921–928. [[CrossRef](#)] [[PubMed](#)]

21. Mahmud, M.S.; Buys, Y.F.; Anuar, H.; Sopyan, I. Miscibility, Morphology and Mechanical Properties of Compatibilized Poly(lactic Acid)/Thermoplastic Polyurethane Blends. *Mater. Today Proc.* **2019**, *17*, 778–786. [[CrossRef](#)]
22. Oliaei, E.; Kaffashi, B.; Davoodi, S. Investigation of structure and mechanical properties of toughened poly (L-lactide)/thermoplastic poly (ester urethane) blends. *J. Appl. Polym. Sci.* **2016**, *133*, 43104. [[CrossRef](#)]
23. Jaso, V.; Cvetinor, M.; Rakic, S.; Petrovic, Z.S. Bio-plastics and elastomers from poly(lactic acid)/thermoplastic polyurethane blends. *J. Appl. Polym. Sci.* **2014**, *131*, 41104. [[CrossRef](#)]
24. Fancey, K.S. Mechanical Model for Creep, Recovery and Stress Relaxation in Polymeric Materials. *J. Mater. Sci.* **2005**, *40*, 4827–4831. [[CrossRef](#)]
25. Lagakos, N.; Jarzynski, J.; Cole, J.H.; Bucaro, J.A. Frequency and Temperature Dependence of Elastic Moduli of Polymers. *J. Appl. Phys.* **1986**, *59*, 4017–4031. [[CrossRef](#)]

Disclaimer/Publisher’s Note: The statements, opinions and data contained in all publications are solely those of the individual author(s) and contributor(s) and not of MDPI and/or the editor(s). MDPI and/or the editor(s) disclaim responsibility for any injury to people or property resulting from any ideas, methods, instructions or products referred to in the content.